

Coulomb blockade versus coherence in transport through a double junction

Ursula Schröter* and Elke Scheer

Fachbereich Physik, Universität Konstanz, Universitätsstraße 10, 78457 Konstanz, Germany

(Received 18 April 2007; revised manuscript received 23 July 2007; published 13 November 2007)

We construct a model describing current transport through a superconducting or normal conducting circuit consisting of two point contacts in series by extending a Green's functions technique. In between the contacts is a mesoscopically large and bulklike island. The model can, in principle, handle contacts in all transmission regimes. Coherent interaction throughout the whole system is included in the form of multiple and multiple Andreev reflections extending over both contacts while accounting for charging effects by a changing electrostatic potential of the island. Our calculations show that even though the onsets of certain current contributions are independent of the island charging energy, Coulomb blockade persists, especially in the normal state. Coulomb staircases can still be visible but get smeared out for particular ratios of the charging energy and the gap in the superconducting state. However, as a general trend, we find that including coherent coupling across the island does not very significantly change the shape of the current-voltage curves compared to the incoherent results.

I. INTRODUCTION

For electric circuits with microscopic islands, thus sufficiently small capacitances, the quantization of charge manifests itself by the phenomenon of Coulomb blockade.¹ Transport through quantum dots in superconducting devices has extensively been studied focusing also on aspects such as even-odd occupation,^{2,3} fractional charge,⁴ and pumping.⁵ Here, we address bulklike metallic islands with negligible intrinsic level spacing of the electronic states. Unlike in Ref. 6 by Kouwenhoven *et al.*, this is mostly not the case for quantum dots for which then a single-level picture is appropriate.^{5,7-9} The contacts, although presenting barriers of the order of the quantum resistance $R_k = h/2e^2$, are not necessarily tunneling junctions but can as well be point contacts and, for example, be arranged with break junctions.¹⁰ These accommodate few transport channels with varying transmission probabilities. This implies that multiple-reflection corrections and, in the superconducting state, multiple-charge transport processes in the form of Andreev reflections play an important role. The transport properties of setups in which such junctions of arbitrary transmission get combined with islands sensitive to single-electron charging are not yet fully understood, the principal question being whether Coulomb blockade suppresses multiple Andreev reflections (MARs) or vice versa.^{8,11} A charging-energy threshold on the Josephson current across a quantum dot has recently been predicted.¹²

We recently presented a model for calculating current-voltage (I/V) characteristics of a double-junction circuit with a metal island. In Ref. 13, we assumed that coherence was not maintained across the island from one junction to the other, which should be correct, if the two contacts are far apart. One could, however, place the junctions close to each other such that quantum coherence is not lost between them. Here, we show how our method can be altered and extended to this situation. The model from Ref. 13 included for each junction in themselves coherent MAR processes together with changes of the island charge, but we shall refer to it for short as the “incoherent” model. The model presented now

and keeping coherence between the contacts is called “coherent.”

The setup considered is shown in Fig. 1(a). An island is linked to a left and a right electrode by quantum-point contacts. Each contact has a capacitance C_i , and the potential of the neutral island is determined by the divider, made up of these two, when a transfer voltage V is applied between left and right. The island potential may further be continuously altered, however, by inducing charge via a gate capacitance. At variance to Ref. 13, we here only consider junctions with a single transport channel each. Our model is made for all three regions L , I , and R of the same material, which has gap

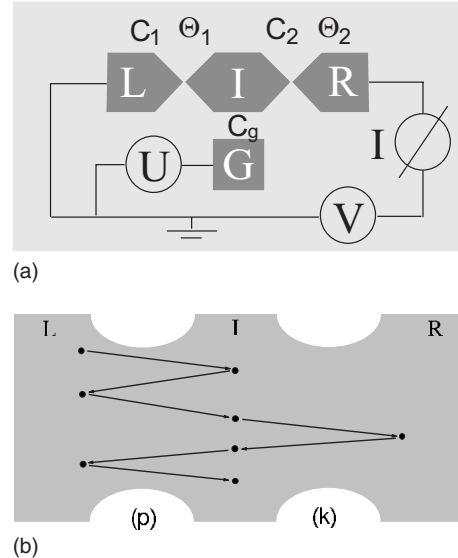


FIG. 1. (a) Setup: island connected to a left and a right lead between which a transport voltage V is applied. Each junction is characterized by a capacitance C_i and a transmission θ_i . The island can further be tuned via a gate capacitance C_g with voltage U . The net current I is the quantity to deduce. (b) Multiple-reflection process extending over both junctions. Effectively transported charges across each junction are counted by p and k .

parameter Δ for the superconducting state. The latter works with a BCS density of states, which collapses to a constant density of states (DOS) with occupied electron states below and empty ones above the Fermi energy in the normal conducting limit $\Delta \rightarrow 0$. No spin polarization^{7,14,15} is considered, and the system is treated at zero temperature. Furthermore, the island is sufficiently large such that a small number of excess electrons or holes do not influence the form of the DOS. The charge determines the Fermi level with respect to the lead potentials. An example of a multiple-reflection process extending over both junctions is depicted in Fig. 1(b). We include multiple Andreev reflections but neglect Cooper-pair tunneling.¹⁶ Herewith, the assumptions for the model are concluded.

We consider our model as realistic for possible realizations of mesoscopic systems. However, the interest of the present paper is not a direct comparison to experiment but a demonstration of conceptual feasibility. The combination of Green's functions and rate equations allows us to treat coherent interaction through the double junctions with bulky island for the low,¹⁷ intermediate, and high-transmission regimes. In Sec. II, we briefly present the extensions of the formalism needed for the coherent case. A selection of example calculations of current-voltage characteristics is presented and discussed in Sec. III before summarizing the results in Sec. IV.

II. GREEN'S FUNCTIONS AND RATE EQUATIONS

Maintaining coherence in transport across the island, there is only one Hamiltonian containing all three reservoirs and both couplings over junctions,

$$H = H_L + H_I + H_R + \sigma_{L \leftrightarrow I} + \sigma_{I \leftrightarrow R}. \quad (2.1)$$

For the transfer Green's function T , which is a 3×3 matrix in site space, we have to solve the Dyson equation,

$$T = (\sigma^1 + \sigma^2) + (\sigma^1 + \sigma^2)gT. \quad (2.2)$$

By σ^1 and σ^2 , we denote couplings across the left and right junctions, respectively. g is the Green's function of the uncoupled sites L , I , and R . T is transformed to Fourier space through

$$T^{n_1 n_2}(\tau, \tau') = \sum_{k+p=n_2-n_1} \int d\omega e^{-i\omega\tau} T_{kmp}^{n_1, n_1+k+p}(\omega) \times e^{-ikA\tau} e^{-im(n_1, k, p)B\tau} e^{-ipC\tau} e^{i\omega\tau'}, \quad (2.3)$$

with A and C being the potential differences of the neutral island to the leads, B proportional to the charging energy $E_c = e^2 / (C_1 + C_2 + C_g)$, and k , m and p are integers. T mediates between the island state with initial and final excess charges n_2 and n_1 . By building two couplings into the Green's function successively,¹⁸ and following Refs. 13 and 19 to construct T through recursions in k and p for the coherent model, Eq. (2.2) can be solved in two steps. Regarding solely coupling across the left junction, in a first step, an intermediate function T^1 fulfilling

$$T^1 = \sigma^1 + \sigma^1 g T^1 \quad (2.4)$$

is calculated, which then enters the second-step equation,

$$T = T^1 + \sigma^2 + T^1 g \sigma^2 + \sigma^2 g T + T^1 g \sigma^2 g T, \quad (2.5)$$

where now only the coupling across the right junction gets newly introduced. Equation (2.2) can alternatively be solved by direct inversion for not too high maximum values of k and p ,

$$T = [1 - (\sigma^1 + \sigma^2)g]^{-1}(\sigma^1 + \sigma^2). \quad (2.6)$$

A special procedure to evaluate inverse matrices of the form $(1-M)^{-1}$ from the electronic supplement of Ref. 18 has been adapted to this problem.

The formula giving the rate by which the island charge is changed between n and $n+1$ by a transfer through a junction (channel) expressed with G_{+-} remains the same as in Ref. 13, however, with G 's now 3×3 matrices in site space, more terms occur when rewriting it using T . For the right junction, as an example, we get

$$\begin{aligned} & 2 \operatorname{Re} \sum_{n'} \{ (\sigma_{RI}^{n+1, n'} G_{IR,+-}^{n', n+1})_{hh} + (G_{RI,+-}^{n, n'} \sigma_{IR}^{n', n})_{ee} \} \\ & = 2 \operatorname{Re} \{ (T_{RI}^r g_{II}^{+-} T_{IR}^a g_{RR}^a)_{hh}^{n+1} + (g_{II}^r T_{IR}^r g_{RR}^{+-} T_{RI}^a)_{hh}^n \\ & \quad + (T_{RL}^r g_{LL}^{+-} T_{LR}^a g_{RR}^a)_{hh}^{n+1} - (T_{LR}^r g_{RR}^{+-} T_{RL}^a g_{LL}^a)_{hh}^{n+1} \\ & \quad + (g_{RR}^r T_{RI}^r g_{II}^{+-} T_{IR}^a)_{ee}^n + (T_{IR}^r g_{RR}^{+-} T_{RI}^a g_{II}^a)_{ee}^{n+1} \\ & \quad + (g_{RR}^r T_{RL}^r g_{LL}^{+-} T_{LR}^a)_{ee}^n - (g_{LL}^r T_{LR}^r g_{RR}^{+-} T_{RL}^a)_{ee}^n \}, \quad (2.7) \end{aligned}$$

where n or $n+1$ denotes the outer charge index of a product. The $T_{LR/RL}$ functions represent an effective coupling between not directly connected sites.²⁰ As all multiple (Andreev) reflection processes are broken down into single-charge hoppings entering the rate terms [Eq. (2.7)], a rate matrix R is constructed solely from $\Delta n=1$ island-charge changes, adding processes from both junctions. With \vec{P} denoting the vector composed of P_n , the probabilities for the island to have n excess charges on it, stationary state requires

$$\frac{d}{dt} \vec{P} = R \cdot \vec{P} = 0. \quad (2.8)$$

With the P_n obtained from Eq. (2.8), the current (dc) is easily calculated using charge transport rates for any single junction.

III. RESULTS

In Fig. 2, we show an IV for the normal conducting case (with finite E_c) for medium transmissions of the junctions. The respective result without coherent interaction between both junctions¹³ is also plotted. In the incoherent model, current onset is at $eV=2E_c$, and further jumps in the derivative are found at $eV=(4n+2)E_c$ — for the symmetric case with equal junction capacitances. In the coherent model, we obtain nonzero current at lower voltages. However, finite current at infinitely small voltage merely occurs in the limit of vanishing E_c , in accordance with the picture of an Ohmic resistance. Otherwise, a Coulomb blockade regime persists.

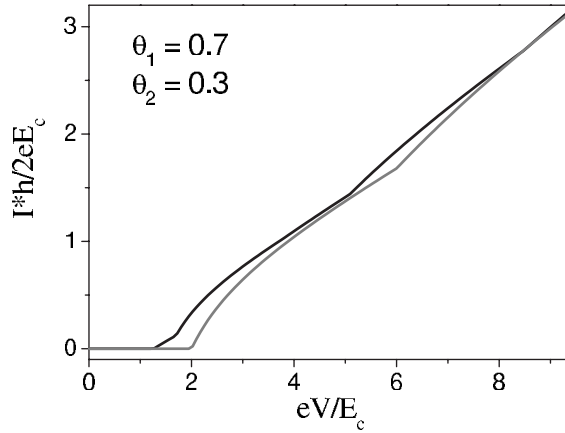


FIG. 2. Normal-state IV curves for symmetric junction capacitances $C_1=C_2$, no gate voltage $U=0$, and transmissions $\theta_1=0.7$ and $\theta_2=0.3$. The light gray curve is the result of the model from Ref. 13.

The lowest possible voltage threshold for current onset is at $eV=\frac{2}{3}E_c$ for maximally open channels $\theta_1=\theta_2=1.0$. We regard setups with the same junction transmission amplitudes t_1 and t_2 in the incoherent and the coherent model.²¹ Depending on θ_1 and θ_2 , the coherent model can yield a greater current than the incoherent one, but it is also possible for the

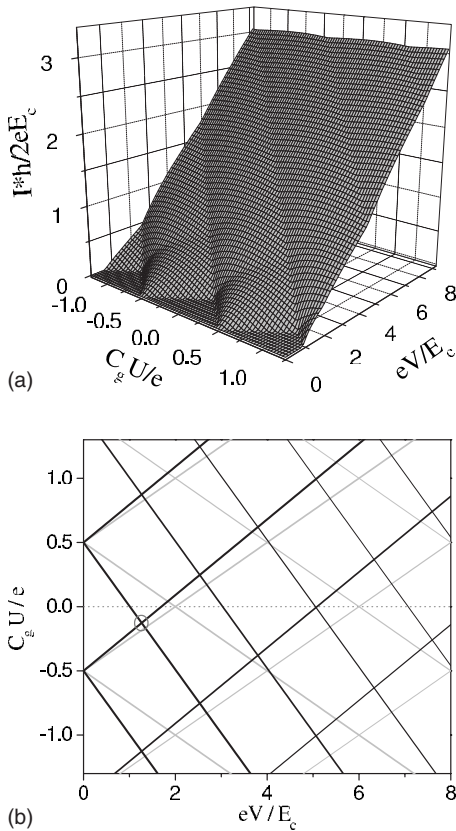


FIG. 3. (a) Current I from coherent model drawn as a function of both transport voltage V and gate voltage U . (b) Lines marking the edges of the Coulomb diamonds (jumps in dI/dV or dI/dU) in the coherent (black) and the incoherent (gray) model. Parameters for both (a) and (b) are the same as in Fig. 2.

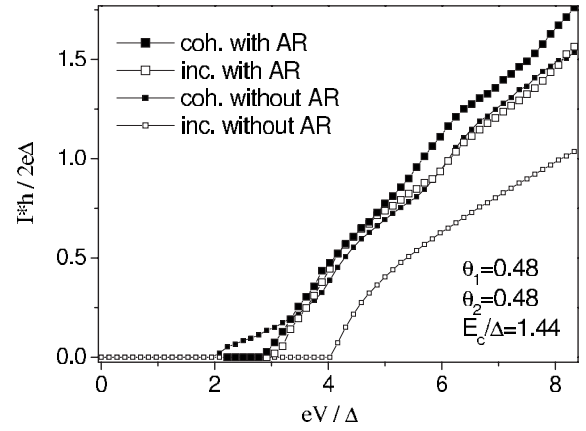


FIG. 4. Calculated IV for equal transmissions, $C_1=C_2$, $U=0$ for $E_c>\Delta$. Current is zero in calculations with Andreev reflection at low voltages where no (big) symbols are drawn.

coherent curve to drop below the incoherent toward larger voltages. Both models fall together in the limit of two very small transmissions as expected and required for consistency. The current as a function of both the transport and the gate voltage [Fig. 3(a)] in the coherent model exhibits Coulomb diamonds like in orthodox theory¹ or in the incoherent model. In the UV plane, the lines marking their edges are not the same though [Fig. 3(b)], and in the coherent case, the slopes are no longer determined by the capacitances alone but depend on the junction transmissions as well.³ One will, nevertheless, not be able to tell whether transport is incoherent or coherent from the shape of $I(V)$ or $I(U)$. The fact that the edges' first crossing point [see Fig. 3(b)] is not found at $U=0$ for the coherent case is of no help, as this would happen for $C_1\neq C_2$ in the incoherent case, too. With slightly different parameters C_1 , C_2 , t_1 , and t_2 — usually not independently known in experiment — it is possible to deduce the same IV from both models.

In Figs. 4–6, we show example calculations for the superconducting state. Here, also IV s containing processes of the kind from Fig. 1(b) are compared to the case where coherent interaction between the two junctions is switched off. In Fig. 4, for medium transmission of both junctions and E_c greater than Δ , we see that with full coherence, the current onset is at slightly lower voltage than $eV=2E_c$, where it was in the incoherent model. At higher voltage, we obtain a somewhat larger current. However, there is no prominent difference in the IV -curves from both models.

In order to provide evidence for direct lead-to-lead transport in the coherent case, we therefore investigate the artificial situation that Andreev reflection (AR) is turned off despite keeping the density of states with the gap from the superconducting state. This is easily done in our formalism. With only electron or hole transfers, current onset would be at $eV=4\Delta$ (for the symmetric case $C_1=C_2$) in the incoherent model, whereas the coherent case would give nonvanishing current starting already at $eV=2\Delta$. The independence of this contribution of the island charge can be proven by repeating the calculation without AR for different gate voltages U . The onset is always found at $eV=2\Delta$ as long as U does not enable

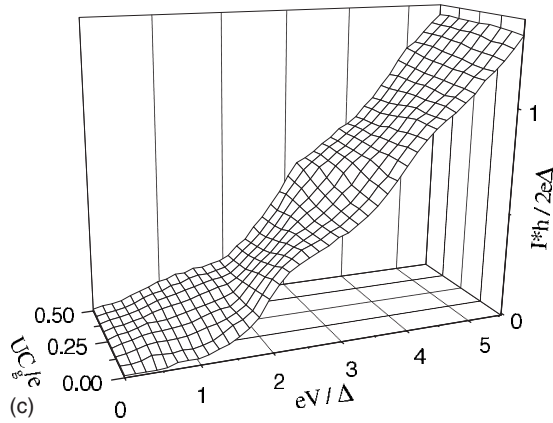
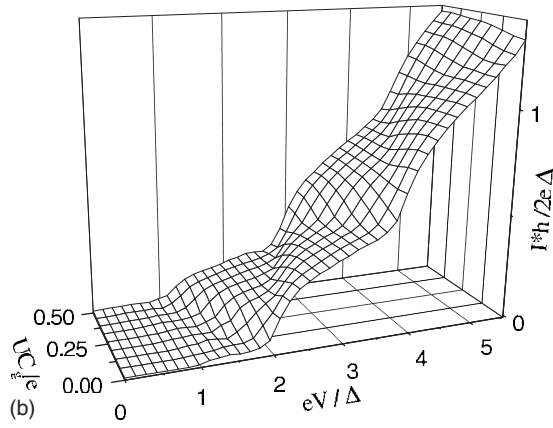
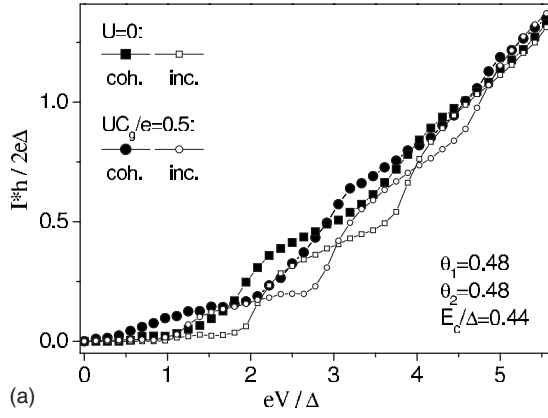


FIG. 5. Calculated IV for the same transmissions, as in Fig. 4, also equals capacitances, but $E_c < \Delta$, slightly below $\Delta/2$. (a) IV curves for U at the beginning and middle of a period in gate voltage for both models. (b) I as a function of V and U for half a period in gate voltage from *incoherent* model. (c) Same as (b) for *coherent* model.

sequential transport at lower voltage. In the full calculation with AR, except for a slightly shifted onset and a rather small enhancement in current, there is not much difference between the IV -curves from the coherent and the incoherent models for any gate voltage U . Back-transport of charges from the island by MAR across a single junction hinders net current from coherent lead-to-lead coupling.

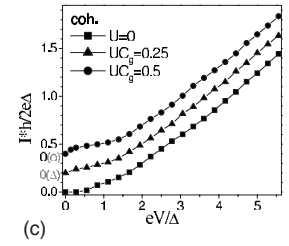
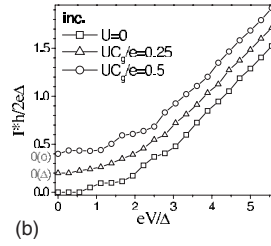
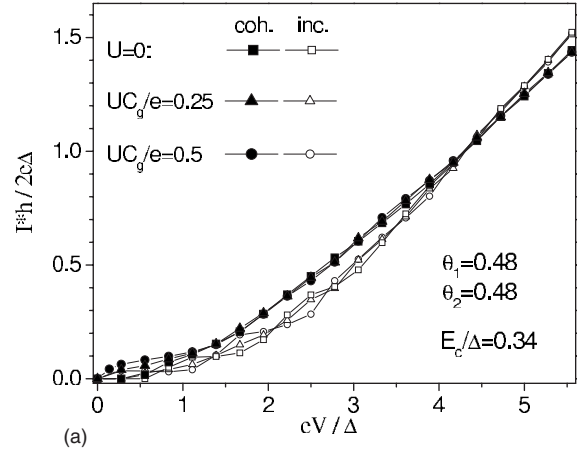


FIG. 6. IV for three different U for equal medium transmission of both junctions, equal capacitances, and E_c about one-third of Δ . All curves are put together in (a) to show where the ones drawn with full symbols nearly fall together and exceed those drawn with open symbols. The same curves from the incoherent and the coherent model are also shown separately and shifted (0.2 units per curve, all have $I=0$ for $V=0$) for different U in (b) and (c) to see their individual shapes.

For both junctions of medium transmission and E_c less than Δ [Fig. 5(a)], even the incoherent model produced little current below $eV=2\Delta$ (for $U=0$) due to MAR in each single junction. $U \neq 0$, of course, shifts the marked current rise from $eV=2\Delta$ — due to first-order AR here with the double junction — to lower voltage. The coherent model for all gate voltages shows a distinct current rise at smaller voltages and a greater current than the incoherent one in the subgap range below roughly $eV=4\Delta$. Plotting I from the incoherent model as a function of V and U , we clearly recognize a Coulomb diamond pattern [Fig. 5(b)]. The steps get smoothed out, but remain visible, in the coherent model [Fig. 5(c)]. Part of the current is now carried by coherent transport from lead to lead, for which voltage thresholds do not depend on the island charging energy.

In Fig. 6, we show IV -curves, again for equal medium transmission of both junctions, but still lower charging energy, for three different gate voltages. Here, the increase in current of the coherent as compared to the incoherent model is such that the step structure gets lost. Curves without coherent coupling between junctions (open symbols) have some visible steps in the range up to about $eV=4\Delta$, at least for gate voltages $U=0$ and $UC_g=e/2$, where crossings of edges of Coulomb diamonds and their subedges from AR occur. For small E_c , the step structure rather quickly becomes too weak to be seen toward higher V , even in the incoherent

case. The important point, however, is that, in the coherent model (full symbols), all IV -curves for different gate voltages almost coincide beginning at a voltage even below $eV = 2\Delta$. This indicates that a transfer mechanism dominates, which does not depend on the charging state of the island, namely, direct coherent lead-to-lead transport. The curves only split for very small V .

Current contributions from coherent transport through both junctions, which add to incoherent processes, become negligible in the subgap regime if one junction has a considerably smaller transmission than the other because the lower-transmission junction then presents a bottleneck and the IV -curves from both models differ less from one another than in the shown examples. Regardless of the ratio E_c/Δ or the transmissions, we do not find signs of crossed AR in the IV characteristics. By expanding terms in Eq. (2.7) into series of powers of σ , one can show that counteracting multiple-reflection corrections are stronger.

IV. SUMMARY

A Green's function formalism known to quantitatively describe transport through a single quantum-point contact, especially with medium or high-transmission channels, in combination with rate equations has been extended to model two such junctions in series. The enclosed island is treated as bulk material, however, sensitive to single-electron charging. Our model further includes a gate electrode. The island potential changing with time is not a principal hindrance for keeping quantum coherence over the whole system, which is the premise set differently here from our previous work.¹³ The two couplings corresponding to the two junctions are of equal importance and built into the Green's functions without approximation.

From our model calculations applied to the normal conducting state, we find that allowing to maintain coherence in transport across the island does not remove the Coulomb

blockade regime, although it reduces its voltage range. Characteristic positions in the current-voltage curves like the onset and sudden changes in slope no longer represent multiples of the island charging energy like in orthodox theory, but depend in a more complex manner also on the junction transmissions.

In the superconducting state with coherent coupling between junctions, it can be proven that transport processes exist, even without Andreev reflection, which require the applied voltage to overcome only once the gap 2Δ despite the bridging of the two junctions. Indications for such direct lead-to-lead transport are the smearing out of the Coulomb steps and the independence of current-voltage characteristics of the gate voltage. When assuming bulk properties for the island as for the leads, sequential, incoherent transport processes are always competing. This has for consequence that coherence can only cause additional current above the incoherent model in the subgap regime if the island charging energy E_c is less than Δ . Subgap regime means voltages below $eV=4\Delta$ for the double junction. A larger ratio E_c/Δ seems to favor a current increase at higher voltages. Nevertheless, apart from the mentioned observations, we have to note that, compared to the case without coherent coupling across the island, full coherence does not introduce other prominent features into the current-voltage characteristics, the qualitative shape of which remains very similar. This will render the distinction between incoherent and coherent transport in an eventual experiment extremely difficult.

As an outlook, we remark that for further improving our model, one should include Cooper-pair tunneling, spin polarization, the possibility to have multichannel junctions in the coherent case, or the two contacts being only partially coupled coherently.

ACKNOWLEDGMENTS

We thank the Deutsche Forschungsgemeinschaft and the Landesstiftung Baden-Württemberg for financial support.

*ursula.schroeter@uni-konstanz.de

¹H. Grabert and M. Devoret, *Single Charge Tunneling* (Plenum, New York, 1992).

²M.-S. Choi, M. Lee, K. Kang, and W. Belzig, *Phys. Rev. B* **70**, 020502(R) (2004).

³M. Houzet, D. A. Pesin, A. V. Andreev, and L. I. Glazman, *Phys. Rev. B* **72**, 104507 (2005).

⁴I. A. Sadovskyy, G. B. Lesovik, and G. Blatter, *Phys. Rev. B* **75**, 195334 (2007).

⁵J. Splettstoesser, M. Governale, J. König, F. Taddei, and R. Fazio, *Phys. Rev. B* **75**, 235302 (2007).

⁶L. P. Kouwenhoven, N. C. van der Vaart, A. T. Johnson, W. Kool, C. J. P. M. Harmans, J. G. Williamson, A. A. M. Staring, and C. T. Foxon, *Z. Phys. B: Condens. Matter* **85**, 367 (1991).

⁷M. Braun, J. König, and J. Martinek, *Phys. Rev. B* **70**, 195345 (2004).

⁸E. Vecino, A. Martin-Rodero, and A. L. Yeyati, *Phys. Rev. B* **68**,

035105 (2003).

⁹G. Tkachov and K. Richter, *Phys. Rev. B* **75**, 134517 (2007).

¹⁰E. Scheer, N. Agrait, J. C. Cuevas, A. Levy-Yeyati, B. Ludoph, A. Martin-Rodero, G. Rubio-Bollinger, J. M. van Ruitenbeek, and C. Urbina, *Nature (London)* **394**, 154 (1998).

¹¹A. Levy Yeyati, J. C. Cuevas, and A. Martin-Rodero, *Phys. Rev. Lett.* **95**, 056804 (2005).

¹²M. G. Pala, M. Governale, and J. König, *New J. Phys.*, **9**, 278 (2007).

¹³U. Schröter and E. Scheer, *Phys. Rev. B* **74**, 245301 (2006).

¹⁴M. Tinkham, D. Davidovic, D. C. Ralph, and C. T. Black, *J. Low Temp. Phys.* **118**, 271 (2000).

¹⁵D. Beckmann, H. B. Weber, and H. V. Lohneysen, *Phys. Rev. Lett.* **93**, 197003 (2004).

¹⁶A. Maassen van den Brink, G. Schön, and L. J. Gerlings, *Phys. Rev. Lett.* **67**, 3030 (1991).

¹⁷B. Kubala, G. Johansson, and J. König, *Phys. Rev. B* **73**, 165316

(2006).

¹⁸U. Schröter, Eur. Phys. J. B **33**, 297 (2003).

¹⁹J. C. Cuevas, A. Martin-Rodero, and A. L. Yeyati, Phys. Rev. B **54**, 7366 (1996).

²⁰J. L. D'Amato and H. M. Pastawski, Phys. Rev. B **41**, 7411 (1990).

²¹We prefer to indicate $\theta_i = \frac{4t_i^2}{(1+t_i^2)^2}$ as equivalent parameters, although the explicit calculation of, for example, $|T_{RI}| = \frac{t_2}{1+t_1^2+t_2^2}$ in the normal state in the coherent case indicates a different conversion to renormalized transmission probabilities.